Journal of Applied Sciences and Nanotechnology, Vol. 2, No. 3 (2022)

Journal of Applied Sciences and Nanotechnology

Journal homepage: https://jasn.uotechnology.edu.iq/

Synthesis of Au:TiO_2 Nanoparticles via Laser Ablation in Liquid Deposited on Porous-Si for Improved Spectral Responsivity

[1]Eman M. Suliman*, [1]Uday M. Nayef, [2]Falah A. Mutlak

[1]Applied Physics Branch, Department of Applied Sciences, University of Technology – Iraq

[2]College of Science, University of Baghdad – Iraq

Article information

Article history:
Received: December, 25, 2021
Accepted: April, 22, 2022
Available online: September, 10, 2022

Keywords:
Au:TiO_2,
Nanoparticles,
Laser ablation,
Porous silicon,
Photo-detectors

Corresponding Author:
Eman M. Suliman
as.18.99@grad.uotechnology.com

Abstract

In this study, Au:TiO_2 nanoparticles (NPs) are prepared by using the laser ablation method in liquid at different laser energies (600, 800, and1000 mJ). After that, Au: TiO_2 NPs were deposited on porous-Si(PS). Porous silicon (PS) is synthesized by using the photo-electrochemical etching (PECE) of n-type crystalline Si (c-Si) wafers of (100) orientation. The intensity of the etching current density was (4, 12, and 20 mA/cm^2), with 16% (HF), and the etching time was 15 minutes. The X-ray diffraction (XRD) techniques, scanning electron microscopy (SEM), UV–visible spectrophotometry, and electrical properties are used to characterize the obtained particles. From the photo-detector measurements, the spectral responsivity curves three inclusive regions; the first peak was due to the absorption of UV light by Au: TiO_2 NPs. The second peak was corresponding to the visible light absorption with the PS layer and the third peak was due to the absorption edge of the Si substrate. The higher responsivity of Au: TiO_2 NPs/PS photo-detector was found to be 2.56A/W for specimens prepared at laser energy 800mJ.

DOI: 10.53293/jasn.2022.4558.1125, Department of Applied Sciences, University of Technology

1. Introduction

Nanoparticles are particles with sizes in the range of hundreds of nanometres in the unit, which have lately been attracting comprehensive attention in different fields of physics, material science, and chemistry, as a result of their unique electronic, physical, magnetic, optical properties [1]. Photodetectors, gas sensors, and solar cells devices are all made with these nanomaterials [2–4]. Chemical and physical processes can both be used to generate NPs. Chemical methods were utilized to produce diverse NPs; but, chemical approaches have significant drawbacks (which include toxicity, incompatibility with the environment, and unwanted compounds) that make them inappropriate when compared to physical processes [5-6]. As a physical approach, pulsed laser ablation in liquids (PLAL) is used. The process of removing a portion of material from the surface of a solid after laser irradiation is called laser ablation. This plays an important role in the processing and structuring of materials in many areas of technology [7]. The laser ablation of a solid target immersed in a liquid milieu has become an increasingly important "top down" method for fabricating and producing metallic colloids metal, semiconductors, alloy, and oxide nanoparticles in deionized water and solvents [8-12]. The size and shape, as well as concentration, of NPs could be controlled by altering the wavelength, energy, and pulse duration of the

laser pulse. [13–16]. The major advantage of the PLAL method is that the produced colloids were chemically pure, containing the only target and fluid constituents. The produced particles are surface-charged as a result of the laser ablation, which is another advantage of the approach. This prevents them from aggregating and ensures the generated colloid's long-term stability (for some months). The fundamental disadvantage of the PLAL technique is the broader size distribution of the nanoparticles generated compared to nanoparticles produced by chemical methods [17-20]. Therefore, laser ablation in solutions has been comparatively rapid, easy to manipulate, and a cost-effective technology [21-22]. TiO_2 is an n-type semiconductor that has a wide band gap of 3.2 eV. There has been much interest in its basic characteristics and for many applications including solar cells, photodetectors, protective coatings, and gas sensors. [23- 25], due to its outstanding physical and chemical properties. These structures have long-term stability, a large surface area to volume ratio, easy preparation, and low cost [26–29]. The crystalline structure of TiO_2 exists mainly in three forms: rutile, anatase, and brookite [30]. In particular, TiO2 is sensitive to light with wavelengths below 380 nm, which belong to the UV region, due to its broad band gap [31]. Noble metal (e.g. gold (Au) nanoparticles) exhibit more favorable plasmon-dominated optical properties than conventional bulk metal because of the resonance of conducting electrons with the incident light [32-34]. Because the SPR occurs from the excitation of vibration of free electrons in response to the electric field of the electromagnetic radiation of incident light, Au NPs show high absorption in the visible region [35-38]. Au NPs can also be used in a variety of fields, including medicine, sensors, and electronics [39]. Au NPs have attracted much attention due to their unique physical and chemical properties that depend on size and morphology [40]. In the present study, we will describe the successful manufacturing of Au-TiO_2 NPs using the PLAL method of Ti plate in a solution of CTAB at room temp, and the manufacturing of photo-detector by deposited colloidal of Au-TiO_2 NPs on porous silicon by the drop casting method.

2. Experimental Details

2.1. Chemicals and Materials

A pellet of gold (Au) with high purity (>99.9%) was obtained from the central bank in Baghdad, Iraq. Ti was acquired as a powder and then formed into a pellet using a 10-bar hydraulic press. Cetyltrimethylammonium bromide ($C_{19}H_{42}BrN$, Mol. Wt 364.45 g mol).

2.2. Preparation of Au:TiO_2 NPs/PS

The colloidal solution of Au:TiO_2 NPs was prepared by using the pulsed laser ablation method. In the first step, the Au NPs that were synthesized via pulsed laser ablation of the gold plate were put on the bottom of a glass vessel filled with 3 ml of an aqueous solution of cetyl-trimethylammonium bromide (CTAB). The target has been irradiated with a laser beam of different values of energies (600, 800, and 1000 mJ/pulse) with 100 pulses and wavelength (1064 nm). This colloidal solution has become to some extent, colored following the procedure of ablation for confirming Au NPs formation. After that Titanium (Ti) target has been placed in Au NPs solution that has been suspended and ablated by the same laser at a variety of concentrations of the TiO_2 NPs. In the second step: an n-type silicon wafer (100) with a resistivity of 1.5-4 Ω.cm was prepared by the PECE method. PECE was achieved by etching silicon target in 16% Hydrofluoric acid ($HF:C_2H_5OH$) as electrolyte at current density 4, 12, and 20 mA/cm^2 for 15 min. and illuminated by a halogen lamp. Then, the Au:TiO_2 suspension was dropped on PS by the drop casing method.

3. Results and Discussion

Figure 1 shows that the materials' X-ray diffractograms were investigated as a function of (core-shell). Au: TiO_2 NPs specimen was prepared by laser ablation at 800mJ energy of the pulsed laser which was deposited onto porous-Si. This figure indicates that the Si is crystalline in the (100) plane at 2θ =33.3° [41], whereas the X-ray photons diffracted from the PS substrate are apparent on the XRD pattern of the sample at $2\theta = 70^{\circ}$. In all of the samples, the core shows peaks due to (200) reflections corresponding to bulk fcc Au [42]. The diffraction peaks of Au NPs consistents of the usual (JCPDS card No 002–1095). The XRD of the anatase TiO_2 NPs has two characteristic peaks at 37. 8 and 60.56, which were corresponding to the planes of (112) and (204) respectively according to (JCPDS card No. 21-1272) [25].

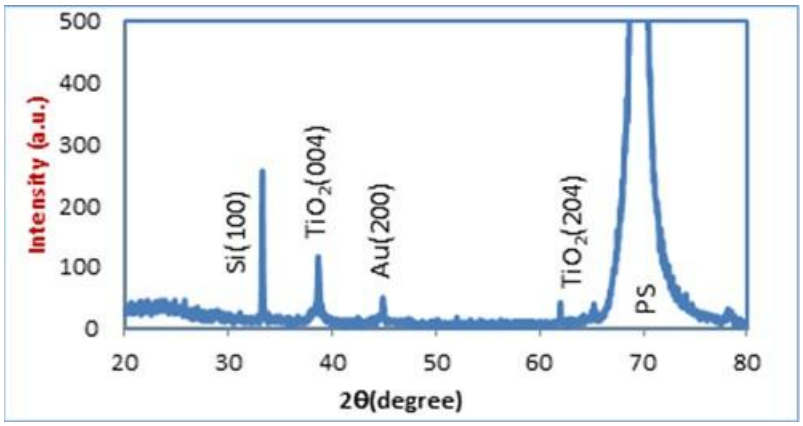

Figure 1: XRD pattern of Au:TiO_2 NPs/PS laser ablated at 800 mJ on PS preparing at etched current 12mA/cm^2 for 15 min. and HF_c 16%.

Figure 2 shows the surface morphology of generated Au: TiO_2 NPs fabricated by PLAL at several energy pulses 600, 800 and1000 mJ that's been deposited on the prepared porous silicon by (12mA\cm^2) etching current density. The ablation using Nd: YAG laser with wavelength 1064 nm. Figure 2-A indicates the regular pores, these small pores begin to form on the Si-layer. Figure 2(B-D) represents Au:TiO_2 NPs/P, which leads to structures that are comprised of spherical and platelet like nanocrystals. There are both isolated particles and agglomerated chains.

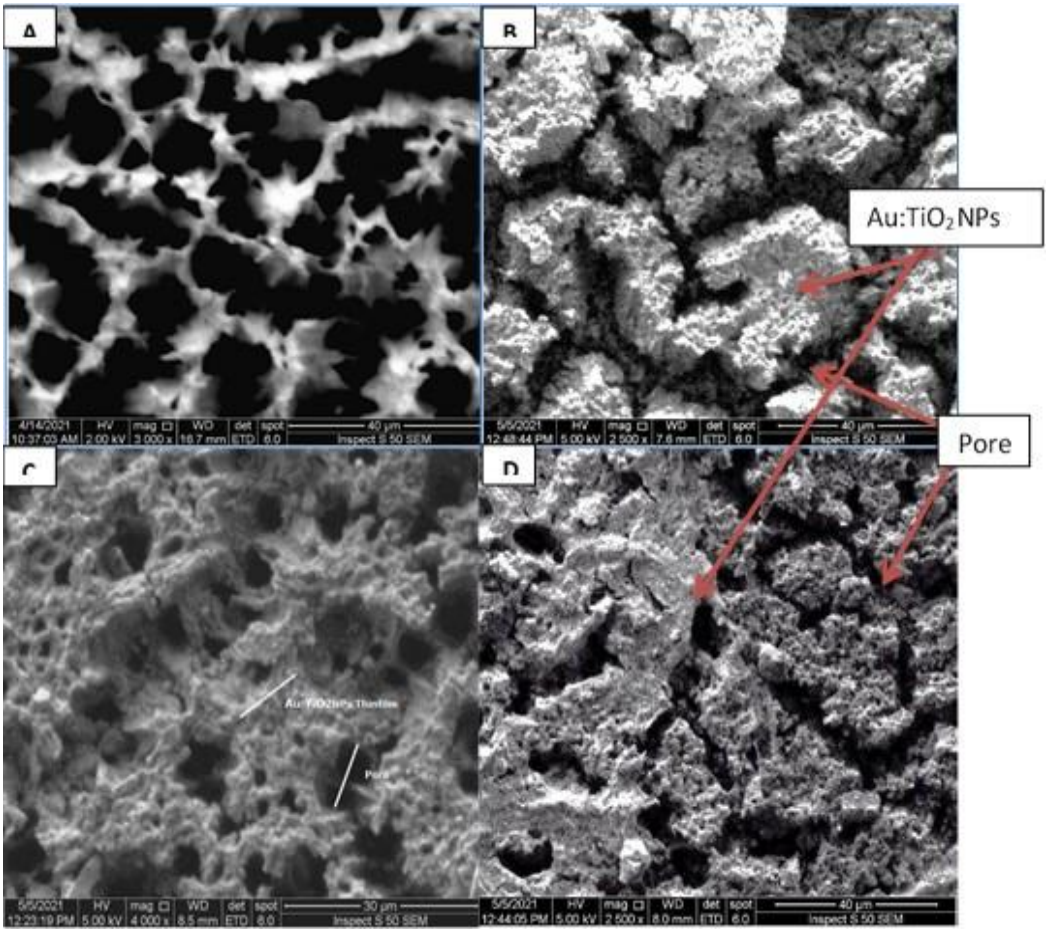

Figure 2: SEM images of Au:TiO_2 NPs/PS (A) PS(12mA/cm^2) (B) Au:TiO_2 NPs laser ablated at 600 mJ (C) Au:TiO_2 NPs laser ablated at 800 mJ (D) Au:TiO_2 NPs laser ablated at 1000 mJ.

From Figure 3, It is observed that the optical absorption ranges of UV-vis. The absorption spectrum of the solution of Au: TiO_2 nanoparticles were produced at various laser energies. The wavelength range between 200-900 nm is used to determine the absorbance of Au:TiO_2 NPs. The spectrum of TiO_2 contains several absorption peaks as observed in Figure 3. The spectrum shows strong absorptions between 200 and 345 nm [43]. UV-vis absorption spectroscopy was used to track the formation of colloids. In organic solvents, the peak maximum corresponding to gold plasmon excitation usually occurs at 512-520 nm [18]. As the gold cluster surface is coated with an oxide layer, the red peak shifts (Figure 1). Shifts in encapsulation and shifts in increasing particle dimension are the two types of shifts. The dielectric constant of the surrounding matrix is related to the shift in plasmon after encapsulation. From Figure 3, it is calculated that the optical band gap Eg of Au: TiO_2 NPs increases with the increase of the laser energy. The energy band gap of the Au: TiO_2 NPs was 4.3, 4.4, and 5.3eV of laser energies (600, 800, and 1000 mJ respectively), which is larger than the 3.2 eV of bulk TiO_2. When the energy of the laser pulses increases (the laser power increases), nanoparticles size decreases, and therefore the energy gap values will increase according to the effects of quantum confinement [44].

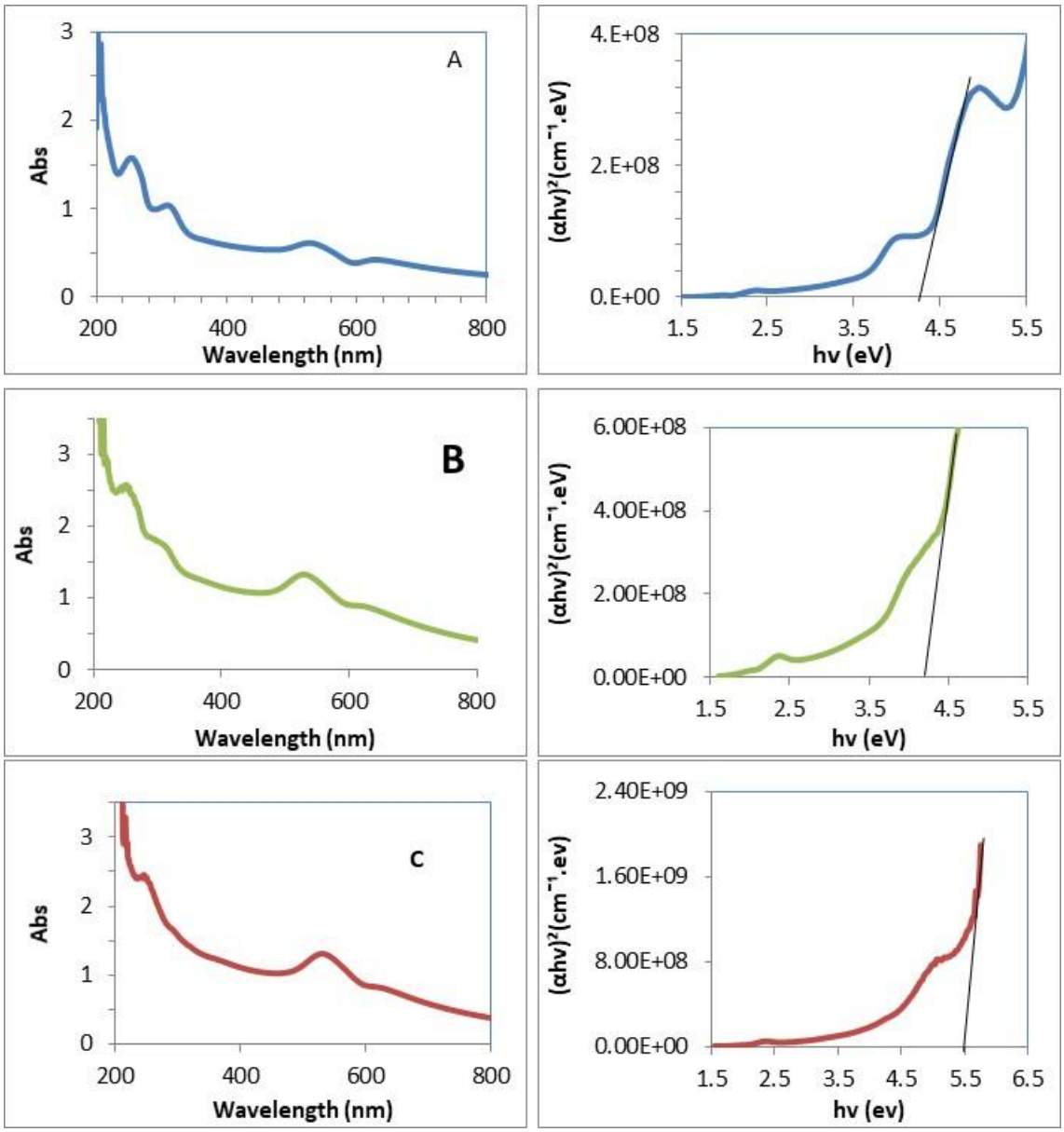

Figure 3: shows absorption of Au: TiO_2 NPs prepared at different laser energy (A) 600, (B) 800, and (C) 1000mJ 100 pulses and laser wavelengths 1064nm, with The energy band gap of Au: TiO_2 NPs.

Figure 4 shows the Current density-Voltage (*I-V*) characteristics in forward and reverse biases of the Al/Au:TiO_2 NPs/PS/nSi/Al in dark surroundings, we found in Figure 4 that there is an increase in the forward current by the increase of voltage (greater 1Volt) and the leakage current decreases (less 1 Volt) because of the resistivity of porous layer decrease. Furthermore, *I–V* measurements show that the Au:TiO_2 NPs/PS samples have the same current density. In this figure, the forward current is divided into two distinct areas. The first area recombination current is established when each electron stimulated from the valance band to the conduction band recombines with a hole in the valance band, increasing the recombination current. The forward current is exponentially enhanced with the applied voltage in the second area at high voltage because this voltage provides enough energy for electrons to exceed the barrier height and the diffusion current to prevail. In the reverse bias, one region exists, it is where the reverse current increases with the applied voltage, and the generated current takes precedence [45].

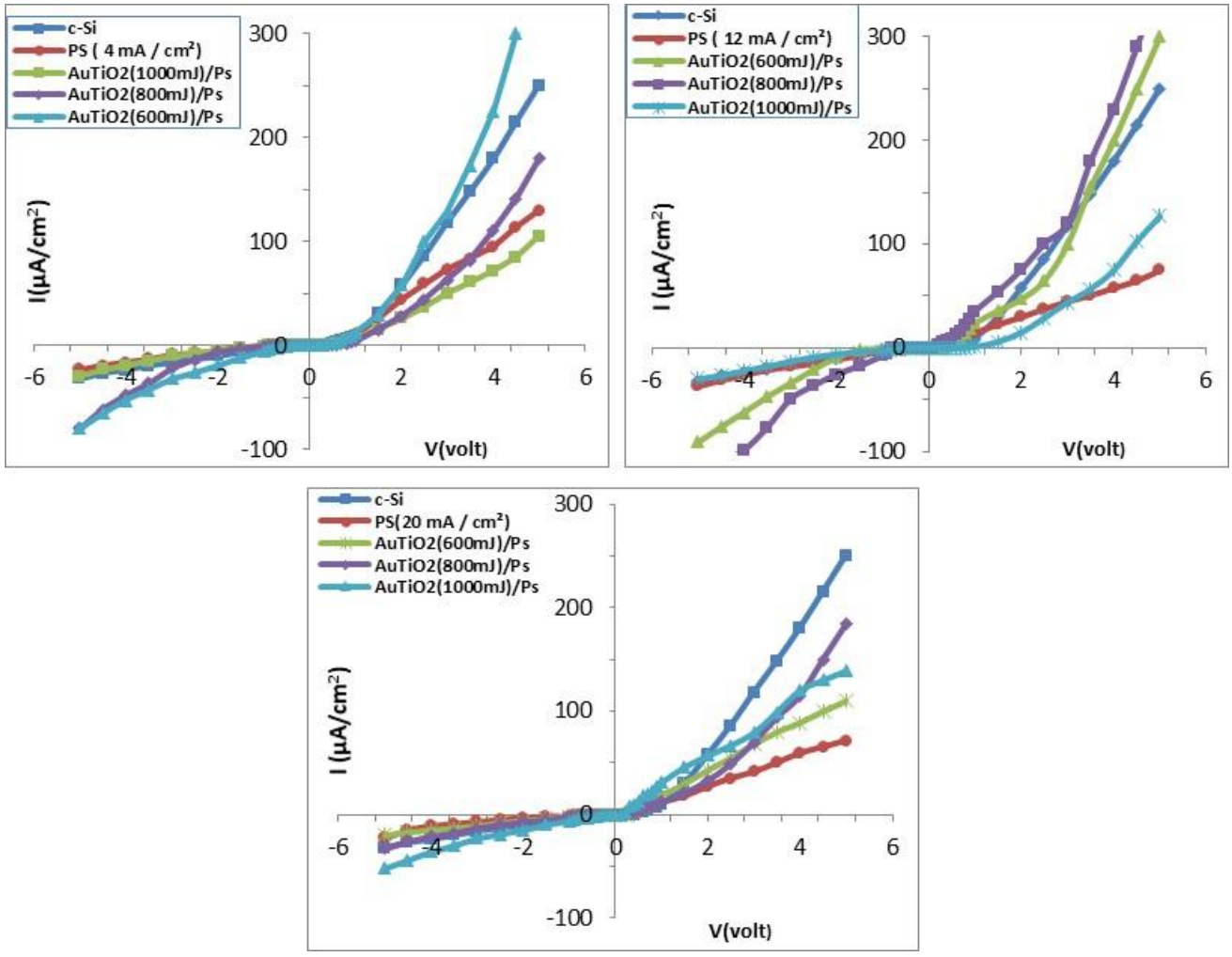

Figure 4: The *I–V* properties of PS and Al/Au: TiO_2 NPs/PS/n-Si/Al preparing at various laser energy and different current densities with fixed etching time (15 min) on the PS layer.

Figure 5 showed the *I-V* characteristics in presence of the light illumination of Al/Au:TiO_2 NPs/PS/n-Si/Al samples fabricated at the same etching time (15 min.) with a constant current density of 12 mA/cm^2 for comparison, using several power intensities. The increase of the reverse bias voltage leads to the increase in the internal electric field which leads to an increase in the probability of the separated electron-hole pairs. Also, the photocurrent increases with the increase of the incident power intensity (5–125 mW/cm^2) due to the increase in the number of the generated photo-carriers in the depletion region [45]. In general, the output currents are decreases when the band-gap increasing for the same light power applied. In the case of Au: TiO_2 NPs/PS samples, there is a higher reverse current density compared to PS due to the conductivity of Au: TiO_2 NPs/PS

layers which were very high. Figure 6 displays the spectral response of the Au:TiO_2 NPs at a bias of 5 V. the responsivity as a function of wavelength for Al/Au:TiO_2 NPs/PS/n-Si/Al samples prepared by laser ablation were deposited on PS layer etched at 12mA/cm^2 current density with 16% HF concentration for 15min. In Figure 6, it is observed that there are three peaks, first region illustrated higher responsivity due to the absorption of UV light 450 nm by Au: TiO_2 NPs. While the second peak refers to the absorption of the visible light region (600-650 nm) for PS, after that the reduction in the responsivity is observed that attributed to the absorption of light by silicon substrate at (750 and 800 nm). The shift in the peak of the response of photodetector toward UV region after the deposit of the Au: TiO_2 NPs ascribed to the enhancement in UV absorption due to a reduction in energy gap [25].

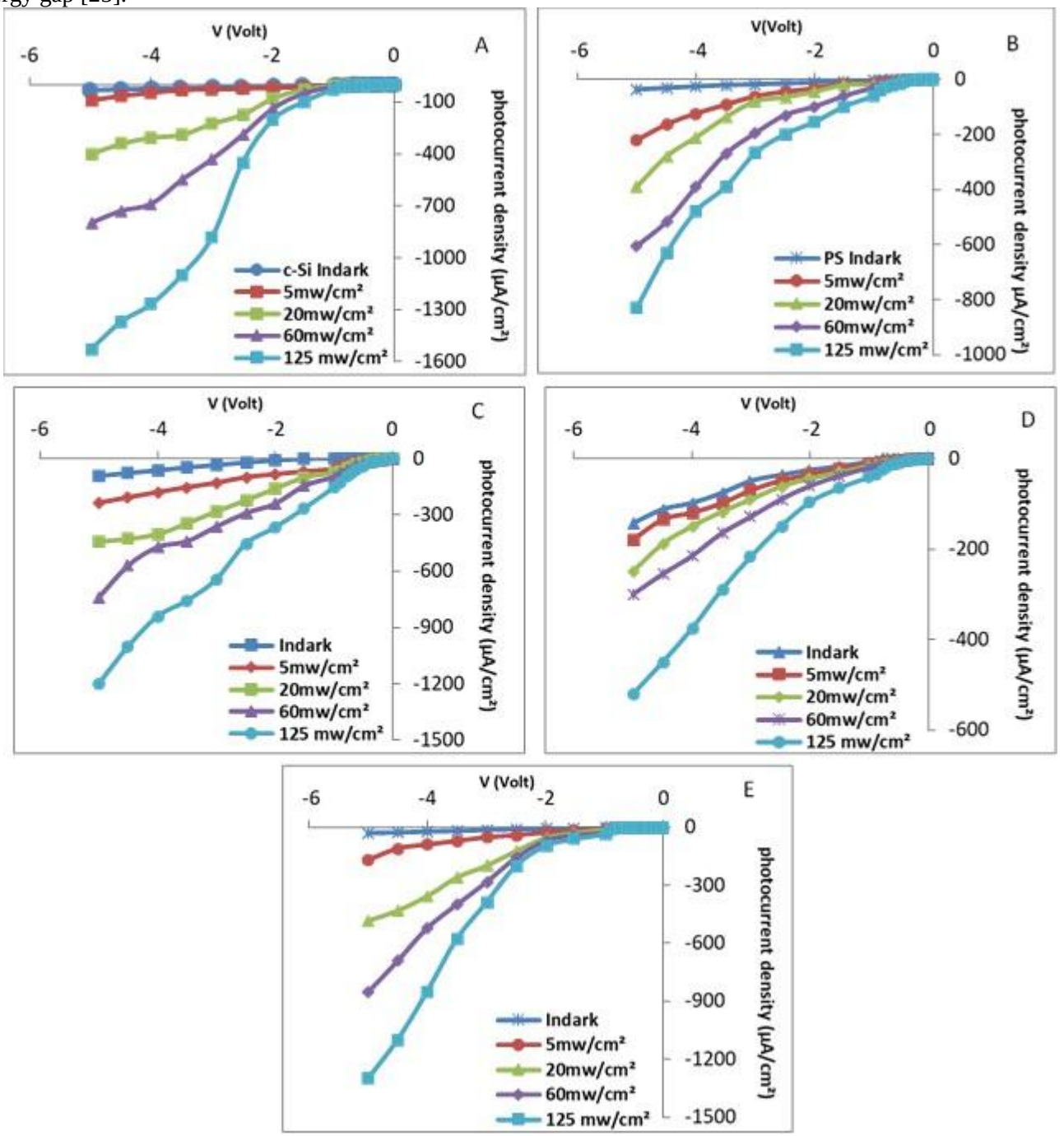

Figure 5: The I_{ph}–V behavior of the applied reverse voltage of (A) c-Si (B) PS etched at 12mA/cm^2 current density with 16% HF concentration for 15min., Al/Au:TiO_2NPs/PS/n-Si/Al with different laser energy (C) 600 mJ, (D) 800 mJ and (E) 1000 mJ.

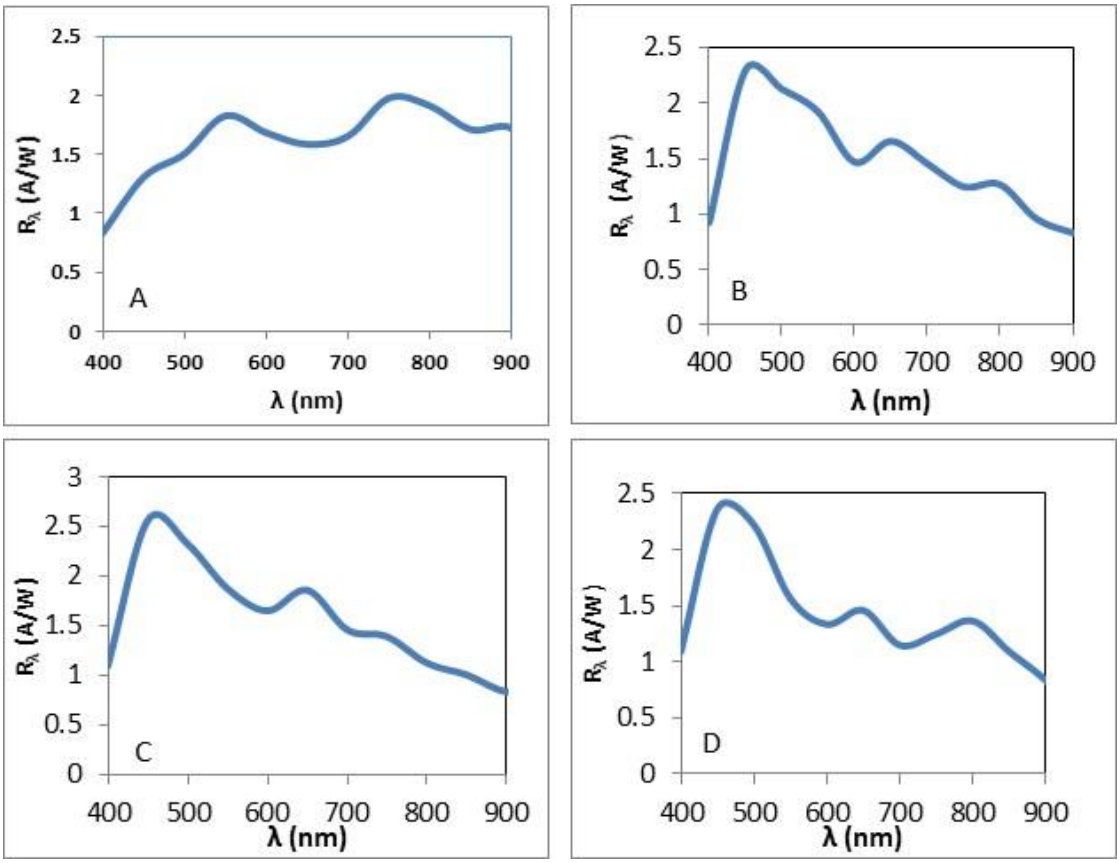

Figure 6: Responsivity of (A) PS and Au: TiO_2 NPs/PS samples at different laser energy ablated (B) 600, (C) 800 and (D) 1000 mJ, 100 pulses with laser wavelength 1064 nm.

4. Conclusions

From this study, it is concluded that the laser ablation of Au:TiO_2 metal in CTAB is considered a promising technique for preparing Au:TiO_2NPs. As deduced by XRD analysis which indicates that the Au:TiO_2 NPs were polycrystalline structure, and optical properties detected that Au:TiO_2 NPS band gap was specified by the quantum size effectiveness. The electrical measurement and photodetectors were strongly dependent on the laser pulse energy. This result improves high responsivity, in the visible region as a photodetector device after we deposited the Au: TiO_2 NPs on porous silicon. The spectral responsivity curves included three regions; the first peak was due to the absorption of UV light by Au:TiO_2 NPs. The second peak corresponds to the visible light absorption with the PS layer and the third peak to the absorption edge of the Si substrate. The best performance of Au: TiO_2 NPs/PS as photo-detector for specimen prepared at laser energy 800mJ were found when the higher responsivity was equal to 2.56A/W.

Acknowledgment

We would like to express our gratitude to the University of Technology and the Applied Science Department in Baghdad, Iraq, for assisting us with this research.

Conflict of Interest

The authors declare that they have no conflict of interest.

References

[1] U. M. Nayef and R. I. Kamel, "Bi2O3Effect of TiO_2 on Enhanced Pyroelectric Activity of PVDF Composite," *Optik*, 208, p.164-146, (2020).

[2] L. Qin, Ch. Shing, and Sh. Sawyer, "Metal–Semiconductor–Metal ultraviolet photodetectors based on zinc-oxide colloidal nanoparticles," *IEEE Electron Dev. Lett*, vol. 32, p.51-53, 2011.

[3] D. Schaadt, B. Feng, Yu E.: "Enhanced semiconductor optical absorption via surface plasmon excitation in metal in nanoparticles," *Appl. Phys. Lett*., vol. 86, p.063106-063109, 2005.

[4] C. Y. Liu, U. Kortshagen.: 'A silicon nanocrystal Schottky junction solar cell produced from colloidal silicon nanocrystals', *Nanoscale Res. Lett.*, vol. 5, p.1253–1256, 2010.

[5] P. V. Kamat, M. Flumiani, and G. V. Hartland, "Picosecond dynamics of silver nanoclusters. Photoejection of electrons and fragmentation," *J. Phys. Chem. B*, vol. 102, p.3123–3128, 1998.

[6] E. A. Inejad and M. H. Mahdieh, "Effect of external electric field on the formation of colloidal Ag–Au alloy nanoparticles through laser post-irradiation," *Journal of Nanophotonics*, vol. 15, p. 026009-1, 2021.

[7] M. I. S. Tan, A. F. Omar, M. Rashid, and U. Hashim,"VIS-NIR spectral and particles distribution of Au, Ag, Cu, Al and Ni nanoparticles synthesized in distilled water using laser ablation." *Results in Physics*, vol. 14, 102497, 2019.

[8] J-Ph. Sylvestre, S. Poulin, A. V. Kabashin, E. Sacher, *et al*.," Surface Chemistry of Gold Nanoparticles Produced by Laser Ablation in Aqueous Media," *J. Phys. Chem. B*, vol. 108, p.16864-16869, 2004.

[9] F. Waag, Y. Li, A.R. Ziefuß, E. Bertin, M. Kamp, *et al*., "Kinetically-controlled laser-synthesis of colloidal high-entropy alloy nanoparticles," *RSC Adv*, vol. 9, p.18547–18558, 2019.

[10] M. Kusaba, M. Hashida, and S. Sakabe, "Extremely low ablation rate of metals using XeCl excimer laser," *J. Laser Micro Nanoeng*. vol. 13, p.17–20, 2018.

[11] D. H. Jwied, U.M. Nayef, F.A.H. Mutlak," Synthesis of C:Se (core:shell) nanoparticles via laser ablation on porous silicon for photodetector application," *Optik*, vol. 231, p. 166493, 2021.

[12] N. A. Abdulkhaleq, A. K. Hasan, U. M. Nayef, "Enhancement of photodetectors devices for silicon nanostructure from study effect of etching time by photoelectrochemical etching Technique", *Optik*, vol. 206, p.164325, 2020.

[13] M. H. Mahdieh and A. Momeni, "From single pulse to double pulse ns laser ablation of silicon in water: photoluminescence enhancement of silicon nanocrystals," *Laser Phys*., vol. 25, p.015901, 2015.

[14] W. Zhang, "Research on successive preparation of nano-FeNi alloy and its ethanol sol by pulsed laser ablation," *Sci. China Ser. B*, vol. 47, no. 2, p.159, 2004.

[15] M. H. Mahdieh and B. Fattahi, "Size properties of colloidal nanoparticles produced by nanosecond pulsed laser ablation and studying the effects of liquid medium and laser fluence," *Appl. Surf. Sci*, vol. 329, p.47–57, 2015.

[16] S. Barcikowski, A. Menéndez-Manjón, B. N.Chichkov, M. Brika, and G.Račiukaitis,"Generation of nanoparticle colloids by picosecond and femtosecond laser ablations in liquid flow," *Applied Physics Letters*, vol. 91, no. 8, p.083113-3, 2007.

[17] S. Barcikowski, G. Compagnini, "Advanced nanoparticle generation and excitation by lasers in liquids," *Phys. Chem. Chem. Phys*., vol. 15, p. 3022–3026, 2013.

[18] R. G. Nikov, N. N. Nedyalkov, A. S. Nikolov, P. A. Atanasov, *et al*, "Formation of bimetallic nanoparticles by pulsed laser ablation of multicomponent thin films in water," *Proc. SPIE 9447, 18th International School on Quantum Electronics: Laser Physics and Applications*, vol. 94470M, 2015.

[19] S. Amoruso, N. N. Nedyalkov, X. Wang, G. Ausanio, *et al*, "Ultrashort-pulse laser ablation of gold thin film targets: Theory and experiment," *Thin Solid Films*, vol. 550, p.190–198, 2014.

[20] A.S. Nikolov, N. E. Stankov, D.B. Karashanov, N.N. Nedyalkov, E.L. Pavlov, *et al*," Synergistic effect in a two-phase laser procedure for production of silver nanoparticles colloids applicable in ophthalmology," *Optics and Laser Technology*, vol. 138, 106850, 2021.

[21] G. Yang, "Laser Ablation in Liquids: Principles and Applications in the Preparation of Nanomaterials," *CRC Press: Boca Raton, FL, USA*, 2012.

[22] A. H. Hamad, K.S. Khashan, A.A. Hadi, D. Yang, "laser Ablation in Different Environments and eneration of Nanoparticles. In Applications of Laser Ablation–Thin Film Deposition," *Nanomaterial Synthesis and Surface Modification*; *Intech Open: London, UK*, p. 177–194 (2016).

[23] N. Janene, A. Hajjaji and M. Ben: Phys. Status Solidi C, 9, (10–11), 2141–2144 (2012).
[24] G. Mital and T. Manoj: Phys. Chem. 56, (16), 1639–1657 (2011).
[25] S. Noothongkaew, J. K. Han, Y. B. Lee, O. Thumthan, and An. Ki-Seok, "Au NPs decorated TiO2 nanotubes array candidate for UV photodetectors," *Progress in Natural Science: Materials International* vol. 27, p. 641–646, 2017.
[26] S. Kathirvel, C. Su, C.Y. Yang, Y.J. Shiao, and B.R. Chen, "The growth of TiO2 nanotubes from sputter-deposited Ti film on transparent conducting glass for photovoltaic applications," *Vacuum*, vol. 118, pp. 17–25, 2015.
[27] J. Lin, M. Guo, C.T. Yip,"High temperature crystallization of free-standing anatasenTiO2 nanotube membranes for high efficiency dye sensitized solar cells," *Adv. Funct. Matter*, vol. 23, pp. 5952–5960, 2013.
[28] V. C. Anitha, B.N. Arghya, S.W. Joo, B. Ki, Min, "Barrier oxide layer engineering of TiO2 nanotube arrays to get single and multistage Y-branched nanotubes: effect of voltage ramping and electrolyte conductivity," *Mater. Sci. Eng. B*, vol. 195, p. 1–11, 2015.
[29] M. Yang, J.L. Zhu, W. Liu, J.L. Sun," Novel photodetectors based on double-walled carbon nanotube Film/TiO2 nanotube array heterodimensional contacts," *Nano Res*., vol. 4, p. 901–907, 2011.
[30] S. M. Hong, S. Lee and H. J. Jung: *Bull. Korean Chem. Soc.*, vol. 34, no. 1, pp. 279–282, 2013.
[31] F. Barreca, N. Acacia, E. Barletta, D. Spadaro, G. Curro and F. Neri: *Appl. urf. Sci.*, vol. 256, pp. 6408–6412, 2010.
[32] X. Pan, Y. Zhao, S. Liu, C.L. Korzeniewski,"Comparing graphene-TiO2 nanowires and graphene-TiO2 nanoparticle composite photocatalysts", *ACS Appl. Mater. Interfaces*, vol. 4, pp. 3944–3950, 2012.
[33] GV. Hartland," Optical studies of dynamics in noble metal nanostructures," *Che Rev*, vol. 111, pp. 3858–87, 2011.
[34] J. Zhu, Du. HF, Q. Zhang, *et al*.," SERS detection of glucose using graphene-oxide-wrapped gold nanobones with silver coating," *J. Mater Chem C*, vol. 7, pp. 3322–34, 2019.
[35] TK. Sau, AL. Rogach, F. Jackel, TA. Klar, and J. Feldmann," Properties and applications of colloidal nonspherical noble metal nanoparticles," *Adv Mater*; vol. 22, pp. 1805–25, 2010.
[36] S. Dash, A. Sikder, and B. Bag, "Phoenix dactylifera (data palm) seed extract mediated green synthesis of gold nanoparticle and it application as acatalyst for the reduction of 4-nitrophenol to 4-aminophenol," *International J. of nanomaterial and biostructure*, (2013).
[37] O. Kvitek, J. Siegel, V. Hnatowcz, and V. Svorcik,"Nobel metal nanostructure influence of structure and environment on their optical properties," *Journal of nanomaterials*, (2013).
[38] U. M. Nayef, I. M. Khudhair, and E. Kayahan, "Organic vapor sensor using photoluminescence of laser ablated gold nanoparticles on porous silicon," *Optik*, vol. 144, p. 546-552, 2017.
[39] W. Ahmed, J. Rnitenbeek," One Step Synthesis of Cetyltrimethylammaniumbromid Stabilized Spherical Gold Nanoparticles," *Journal of Nanosciencewith Advanced Technol*ogy, 2016.
[40] M. Murawska, A.Skrzypczak and M.Kozak,"Structure and morphology of gold nanoparticles in solution studied by TEM, SAXS and UV-Vis" ACTA Phys. Polonica A, (2012).
[41] A. M. Alwan , M. J. Mahmood,"Using Laser Duty Cycles for Modifying the Performance of Au-NPs/Si Nano Column Hot Spot SERS Sensors," *Springer Science+Business Media, LLC, part of Springer Nature* (2020).
[42] R. T. Tom, A. S. Nair, N. Singh, M. Aslam, et al," Freely Dispersible Au@TiO2, Au@ZrO2, Ag@TiO2, and Ag@ZrO2 Core-Shell Nanoparticles: One-Step Synthesis, Characterization, Spectroscopy, and Optical Limiting Properties,*"Langmuir*, vol. 19, p. 9-3445, 2003.
[43] U. M. Nayef, K. A. Hubeatir, and Z. J. Abdulkareem, "Characterisation of TiO2 nanoparticles on porous silicon for optoelectronics application," *Materials Technology: Advanced Functional Materials*, vol. 31, 2016.

[44] H. M Ali, S. A. Makki, and A. N Abd, "Enhanced photo-response of porous silicon photo-detectors by embedding Titanium-dioxide nano-particles," *Journal of Physics: Conf. Series*, vol. 1003 012073, 2018.

[45] U. M. Nayef, K. A. Hubeatir, and Z. J. Abdulkareem, "Ultraviolet photodetector based on TiO2 nanoparticles/porous silicon hetrojunction," *Optik*,, vol. 127, no. 5, pp. 2806-2810, 2016.